VSP migration by single shot record inversion*

J.A. Harwijanto,†** C.P.A. Wapenaar† & A.J. Berkhout†

Vertical seismic profile (VSP) data have been used for many years to obtain *lithological* information from the subsurface in the direct vicinity of the borehole, and to 'calibrate' the seismic processing of surface data (Hardage 1983; Balch & Lee 1984). A relatively unexplored aspect of VSP data is the potential to obtain *structural* information from the subsurface around the borehole. Structural information can be obtained both from surface data and from VSP data by seismic migration. As opposed to surface data migration, however, very few publications on VSP data migration have appeared in the seismic literature. Amongst others, we mention Gazdag & Sguazzero (1983) and Chang & McMechan (1986). Some important complications to be dealt with in VSP migration are the severe variations of the propagation velocity along the borehole, the steep propagation angles (relative to the normal to the borehole) and the sometimes significant deviations of the borehole from the vertical. In this paper we discuss an efficient, wave-equation-based VSP migration scheme which copes with all these problems. The scheme is a generalisation of pre-stack migration by single shot record inversion as proposed by Berkhout (1984).

Geometrical considerations

In this section we discuss VSP migration from a geometrical point of view. For convenience we consider a vertical borehole and a constant propagation velocity c. Although our algorithm is designed to handle complicated configurations, the considerations in this section for a simplified subsurface will support insight into the mechanism of VSP migration.

Consider the 2D VSP configuration shown in Fig. 1a. The borehole is located at $x = 0$, the detectors in the borehole are characterised by the coordinates $(0, z_d)$. The source is located at the surface $z = 0$ at a distance x_s from the well. Furthermore, a diffracting object is present in the subsurface at (x_0, z_0). For the moment we assume that the surface is reflection-free.

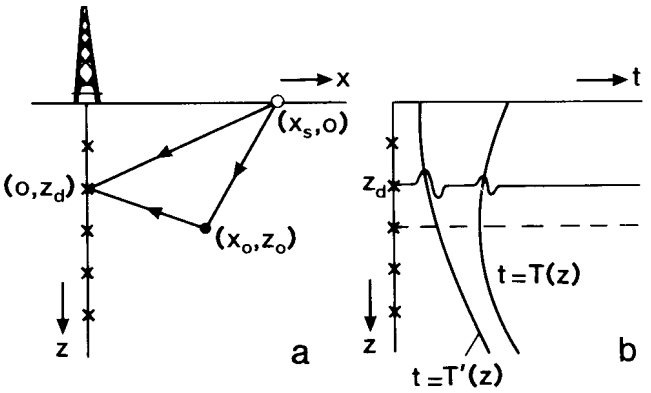

Fig. 1. In VSP data acquisition techniques the detectors are placed in the borehole. (a) Subsurface configuration with point diffractor. (b) Traveltime curves, corresponding to the direct wave (T') and the diffracted wave (T).

The detected field in the well consists of a direct wave and a diffracted wave. The traveltime $t = T'(z)$ of the direct wave is given by

$$T'(z) = \frac{1}{c}\sqrt{x_s^2+z^2}, \qquad (1)$$

and the traveltime $t = T(z)$ of the diffracted wave is given by

$$T(z) = \frac{1}{c}\sqrt{(x_0-x_s)^2+z_0^2}+\frac{1}{c}\sqrt{x_0^2+(z_0-z)^2}. \qquad (2)$$

These traveltime curves describe hyperbolae in the z,t plane as is shown in Fig. 1b.

Let us now consider one seismic trace, registered by a detector at a fixed depth z_d. If we processed this trace by an ideal VSP migration algorithm, then we should obtain an 'image locus' which describes all possible diffractor positions that can cause an observation at $t = T(z_d)$. The equation for this image locus is easily obtained from equation (2) by replacing the variable depth z by the fixed detector depth z_d and by replacing the fixed diffractor coordinates (x_0, z_0) by the variable subsurface coordinates (x,z):

$$T(z_d) = \frac{1}{c}\sqrt{(x-x_s)^2+z^2}+\frac{1}{c}\sqrt{x^2+(z-z_d)^2}. \qquad (3)$$

This equation describes an ellipse in the x,z plane, with foci at $(0, z_d)$ and $(x_s, 0)$, which are the positions of the detector and the source, respectively. This ellipse, which can be seen as the impulse response of the ideal VSP migration algorithm, is shown in Fig. 2a.

*Presented at the 47th EAEG Meeting, Budapest 1985.

†Delft University of Technology, Laboratory of Seismics and Acoustics, PO Box 5046, 2600 GA Delft, The Netherlands.

**Present address: Shell Companies in Indonesia, PO Box 2634, Jakarta 10001, Indonesia.

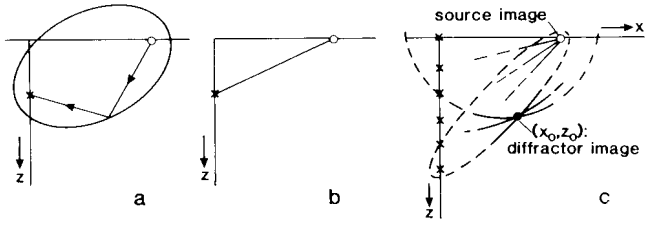

Fig. 2. VSP migration of each detector response yields a so-called 'image locus'. (a) Image locus for the diffracted wave. (b) Image locus for the direct source wave. (c) The superposition of various image loci yields resolved images at the diffractor and source positions.

Assuming that we cannot determine whether an observation represents the direct or the diffracted wave, then the observed event at $t = T'(z_d)$, given by relation (1), will cause a 'ghost image locus', defined by

$$T'(z_d) = \frac{1}{c}\sqrt{(x-x_s)^2+z^2}+\frac{1}{c}\sqrt{x^2+(z-z_d)^2}. \quad (4)$$

This equation describes an 'ellipse', degenerated into a straight line between the source and the detector (see Fig. 2b).

In order to determine the true diffractor position, we need to apply the migration procedure to other traces registered by various detectors at different depths z_d in the well. A superposition of various image loci is shown in Fig. 2c. It consists of many ellipses which intersect at the diffractor position (x_0, z_0), and many straight lines, which intersect at the source position $(x_s, 0)$. Obviously, the migrated direct source wave does not contribute to the image of the diffractor and therefore it should preferably be removed from the data before migration.

So far we have considered primary waves only. Let us now assume that, besides the direct source wave and the diffracted wave, a multiply reflected wave (a 'surface ghost', reflected by the free surface) is present as well. The raypaths are shown in Fig. 3a; the corresponding traveltime curves are shown in Fig. 3b. The polarity of the surface ghost, depicted by the dashed traveltime curve in Fig. 3b, is opposite to the polarity of the diffracted primary arrival. At first glance it seems advisable to remove this downgoing multiply reflected wave from the data together with the downgoing direct source wave because it might produce a ghost image which does not contribute to the diffractor image. However, if the free surface boundary conditions are properly incorporated in the migration algorithm, then the multiply reflected wave may improve the resolution of the diffractor image significantly. This can be explained as follows. Instead of explicitly defining the boundary conditions (zero pressure at the free surface), we may extend the VSP data set to 'negative depths' (above the surface) by copying the traces at the corresponding positive depths and by reversing their polarity (see also Hu & McMechan 1986). The traveltime curves in the extended VSP data set are shown in Fig. 3c (for clarity the direct source wave has been removed). Note that the diffracted primary arrival, depicted by the solid traveltime curve in Fig. 3c, now covers a larger depth range than in Fig. 3b. Migration of all events described by this extended traveltime curve yields a superposition of ellipses which intersect at the diffractor position (x_0, z_0), as is shown in Fig. 3d. Because a wide 'aperture' is used, the 'fan' at (x_0, z_0) covers a wide angle range, which assures a high resolution. Finally, note that migration of all events described by the dashed traveltime curve in Fig. 3c would yield a ghost image with opposite polarity at $(x_0, -z_0)$, which can be easily removed because it does not form part of the subsurface.

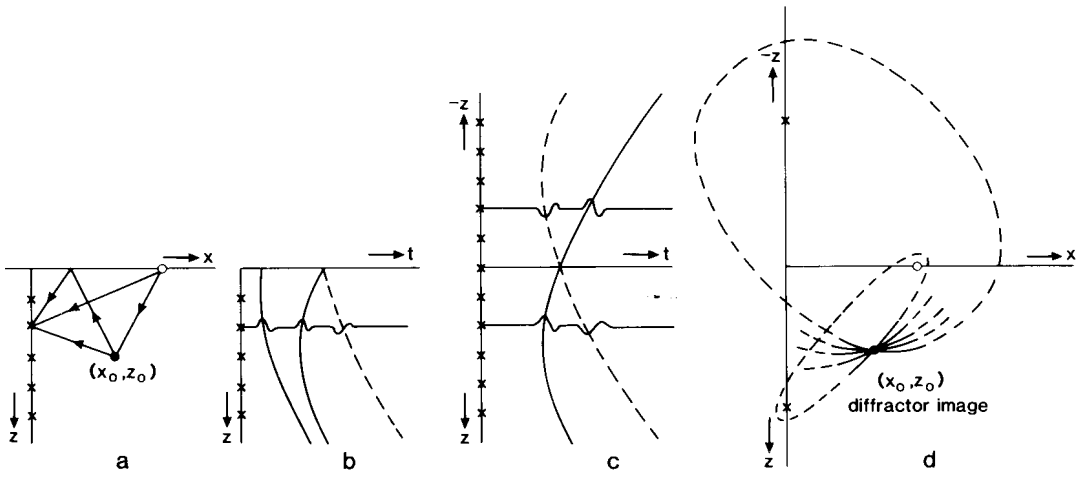

Fig. 3. Surface ghost reflections may improve the resolution of the image significantly. (a) Subsurface configuration, bounded by a free surface. (b) Traveltime curves, including the surface ghost. (c) Extended VSP data set, simulating the free boundary conditions (for clarity the direct source wave has been removed). (d) Migration of the extended VSP data set yields a well resolved image of the point diffractor.

Principle of VSP migration by single shot record inversion

Most seismic migration schemes for surface data consist of two steps:

1. Downward extrapolation of the wavefields from the acquisition surface into the subsurface.
2. Estimation of the subsurface reflectivity distribution from the downward extrapolated wavefields.

The latter step is generally called imaging.

For VSP migration it seems natural to replace downward wavefield extrapolation by lateral wavefield extrapolation, away from the well. However, this is not attractive for various reasons:

(i) Severe propagation velocity variations may occur *along* the recorded profile.
(ii) Steep propagation angles (relative to the extrapolation direction) may occur.
(iii) The acquisition configuration may be very irregular, particularly in case of deviated wells.

Chang & McMechan (1986) show that these problems can be elegantly overcome by carrying out reverse *time* wavefield extrapolation rather than wavefield extrapolation in *space*. However, reverse time migration algorithms are in general quite expensive (both with respect to computation time and required memory space). We prefer to apply wavefield extrapolation in space (either downward or laterally), because it can be applied for each discrete frequency component, which is advantageous both with respect to computation time and required memory space (Berkhout 1984).

The above-mentioned three problems in VSP migration can be overcome if we keep in mind that a VSP data set is built up by carrying out a number of independent seismic experiments (for each experiment a single detector is placed at a new depth in the well and the source is activated at a fixed surface position). Hence, the *basic* experiment in VSP acquisition yields *one* seismic trace, related to one source and one detector position. In the following we discuss VSP migration for each basic seismic experiment. Migration of each basic experiment can be carried out by *downward extrapolation* along the depth axis and imaging. Note the following benefits:

(i) Strong vertical velocity variations can be accounted for when the downward extrapolation is carried out recursively.
(ii) The propagation angles (relative to the extrapolation direction) are moderate.
(iii) Any acquisition configuration is allowed; the independently migrated basic experiments are combined afterwards.
(iv) Downward extrapolation can be carried out efficiently and in a very accurate way in the frequency domain.

We now discuss in more detail the migration procedure for one basic experiment. First of all we remark that we consider migration of upgoing waves only; that is, we assume that the downgoing waves have been removed from the data (optionally after extending the VSP data set to negative depths as described in the previous section), by a velocity filtering procedure (Seeman & Horowicz 1983). The reason for this is that the migrated downgoing source wave would obscure the relevant diffractor and reflector images; furthermore, the migrated downgoing diffracted waves would hardly improve the resolution of the image. We consider the basic configuration, shown in Fig. 4, with one source on the surface at $(x_s, 0)$, and one detector at $(0, z_d)$. The migration procedure for this basic configuration consists of the following steps:

(i) Forward extrapolation of the downgoing source wavefield to depth level z_i (simulation of downward propagation effects).
(ii) Inverse extrapolation of the detected upgoing wavefield to depth level z_i (elimination of upward propagation effects).
(iii) Correlation of the extrapolated downgoing and upgoing waves in the 'imaging area' (overlap area) at depth level z_i.
(iv) At reflectors and diffractors the downgoing and upgoing waves are time-coincident. Hence, 'imaging' can be carried out by extracting the zero-time component of the correlation result, thus obtaining an estimate of the reflectivity distribution at the current depth level z_i.

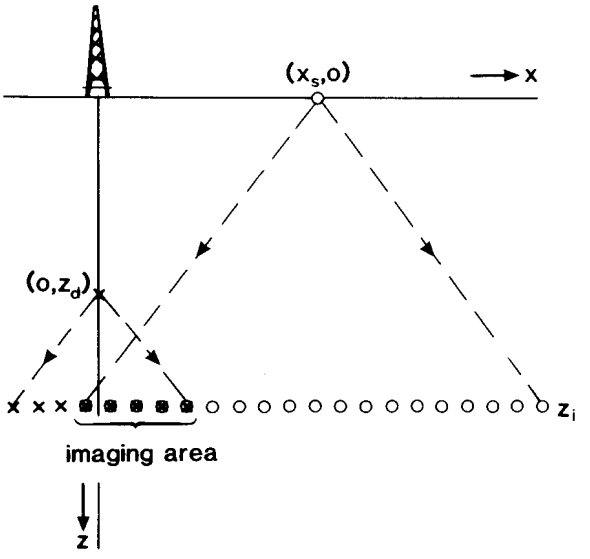

Fig. 4. Migration of a basic VSP experiment consists of the following steps for each imaging depth level z_i: (i) forward extrapolation of the downgoing source wave and inverse extrapolation of the detected upgoing waves to depth level z_i; (ii) imaging in the overlap area by correlating the downgoing and upgoing waves at z_i and by extracting the zero-time component.

The procedure should be repeated for all depths z_i, thus yielding one migrated basic seismic experiment.

Let us now study the mechanism of this migration procedure by considering the same configuration as in the previous section. Ideal forward extrapolation of the point source at $(x_s, 0)$ to depth level z_i yields an impulse response with traveltimes defined by the hyperbolic relation

$$T_s(x,z_i) = \frac{1}{c}\sqrt{(x-x_s)^2+z_i^2}. \quad (5)$$

Ideal inverse extrapolation of the data detected at $(0, z_d)$ (one event at $t = T(z_d)$), yields a time-reversed impulse response with traveltimes defined by the hyperbolic relation

$$T_d(x,z_i) = T(z_d) - \frac{1}{c}\sqrt{x^2+(z_i-z_d)^2}. \quad (6)$$

By equating the traveltimes of both responses

$$\text{i.e. } T_s(x,z_i) = T_d(x,z_i) \quad (7a)$$

so that

$$T(z_d) = \frac{1}{c}\sqrt{(x-x_s)^2+z_i^2} + \frac{1}{c}\sqrt{x^2+(z_i-z_d)^2} \quad (7b)$$

and solving for x, we find those coordinates (x,z_i) where the correlation of the extrapolated downgoing and upgoing waves has its maximum at zero time, which is where the algorithm produces an image. Equation (7b) may have two solutions; hence the algorithm may produce two images at z_i (see also Fig. 5). Note that when we replace the fixed imaging depth z_i in relation (7b) by the variable depth coordinate z we obtain equation (3) again, which describes the elliptical image locus in the x,z plane (Fig. 2a).

So far we have considered VSP migration of one basic seismic experiment (one source and one detector). VSP migration of a VSP data set (one source and many detectors) could in principle be accomplished by migrating all individual basic experiments and by summing all migrated results together afterwards. However, this procedure would be very cumbersome because a complete migration would be carried out for each detected trace. In the practical implementation we took advantage of the fact that the same extrapolation operators are used for each migration. By properly interchanging extrapolation and summation steps, the number of computations required for the migration of a VSP data set can be of the same order as the number of computations required for the migration of one single trace. In Fig. 6 we show a superposition of traveltime curves of different responses (detected at different detector depths z_d) all extrapolated to the same image depth level $z_i = z_0$, where z_0 is the diffractor depth. Notice that each time-reversed 'detector impulse response' has two intersections with the 'source impulse response'. One of these intersections is the same for

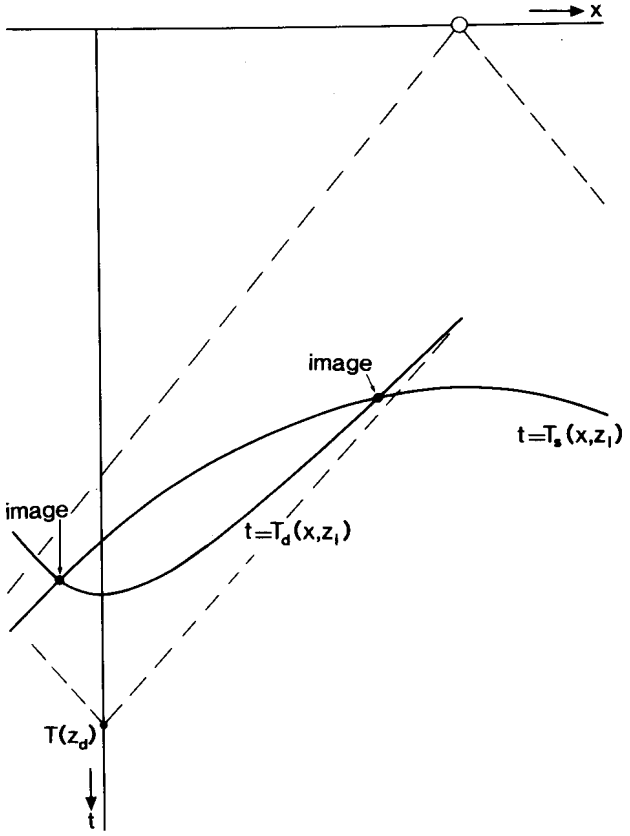

Fig. 5. Traveltime curves at imaging depth z_i, corresponding to the forward extrapolated source data (T_s) and the inverse extrapolated detected data (T_d), related to one basic experiment.

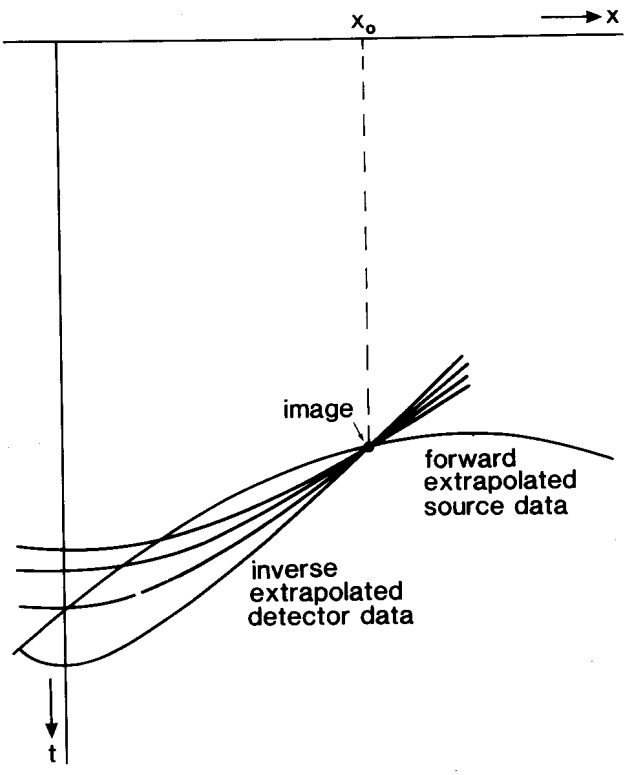

Fig. 6. Superposition of traveltime curves (related to various basic experiments in one VSP data set) at imaging depth $z_i = z_0$, where z_0 is the depth coordinate of the diffractor. The inverse extrapolated detector data all intersect the forward extrapolated source data at $x = x_0$, where x_0 is the lateral coordinate of the diffractor.

each 'detector impulse response' and causes the image at (x_0, z_0).

Finally, if various VSP data sets are available (various sources and many detectors), then each VSP data set can be migrated using the procedure described above ('single shot record inversion') again the individual migration results can be stacked afterwards. The principle is visualised in Fig. 7.

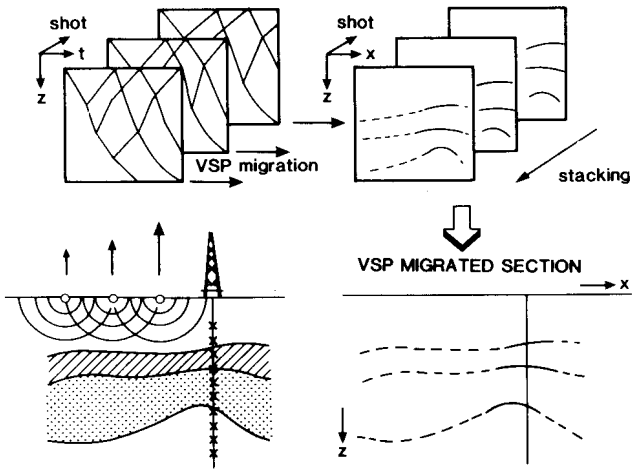

Fig. 7. If various VSP data sets are available they can be migrated individually ('single shot record inversion'), followed by stacking.

Examples

In this section we demonstrate the performance of our VSP migration algorithm. We modelled synthetic VSP gathers for some interesting subsurface configurations. In all the examples we consider VSP migration of primary reflected upgoing waves only.

The first subsurface model contains a faulted layer in an otherwise homogeneous medium with a propagation velocity of 2000 m s^{-1} (see Fig. 8). A vertical well is located at a distance of 800 m from an arbitrary origin. Eight VSP data sets were generated with sources located on the surface at distances from 0 to 700 m to the left of the well with a spacing of 100 m; 49 detectors are equidistantly positioned in the well at intervals of 20 m. Figure 9 shows three representative VSP data sets (upgoing waves only) and Fig. 10 shows the corresponding migration results. Figure 11 shows the stack of eight migration results. Note that the lateral resolution improved compared with the individual migration results (see for instance Fig. 10b). If we include additional VSP data sets with sources located on the surface to the right of the well (from 800 to 2000 m with a spacing of 100 m) then the resolution improves again (see Fig. 12). Note that the final result (Fig. 12c) shows the main features of the subsurface around the well.

In the second model two horizontal layers overlie a pinch-out and an anticline (Fig. 13a). A deviated well

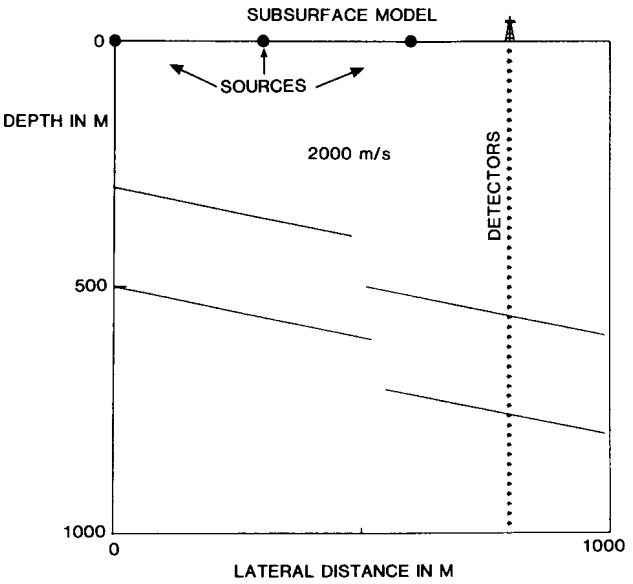

Fig. 8. A model with a faulted layer in an otherwise homogeneous medium. The well is located at x = 800 m.

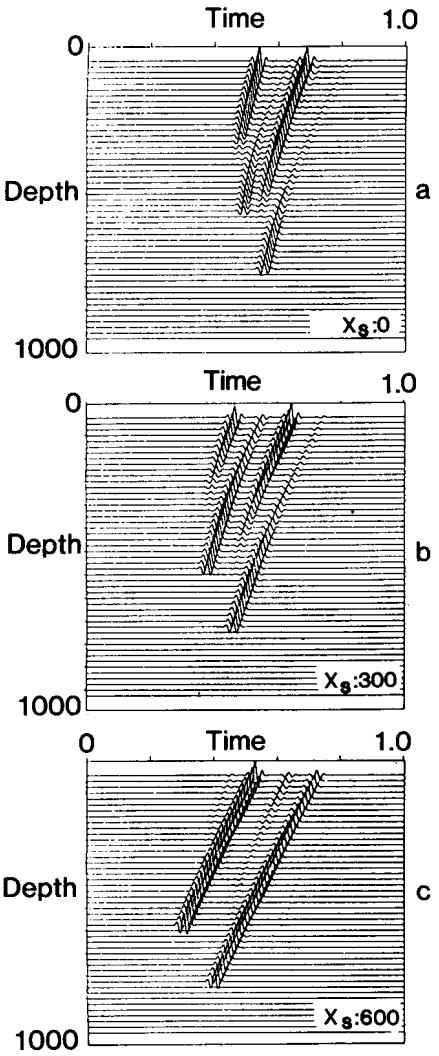

Fig. 9. VSP data sets computed for the model of Fig. 8: (a) source at 0 m; (b) source at 300 m; (c) source at 600 m.

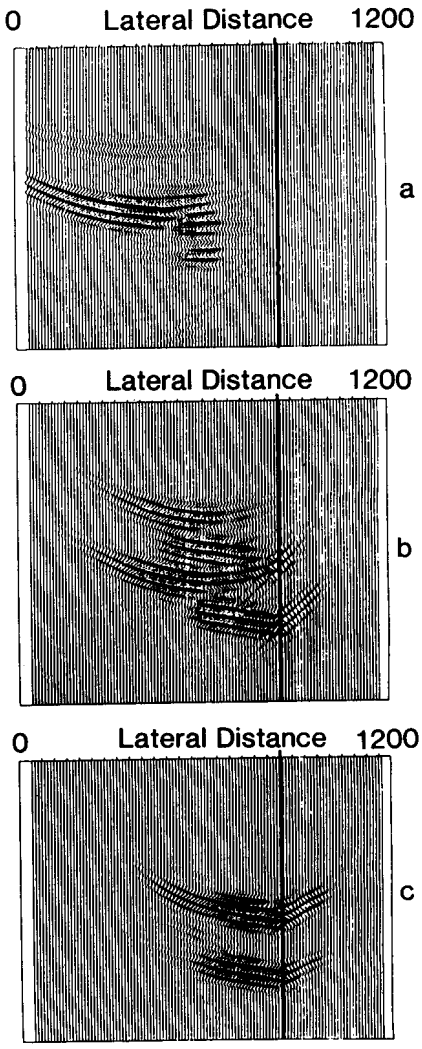

Fig. 10. VSP data sets of Fig. 9 after migration.

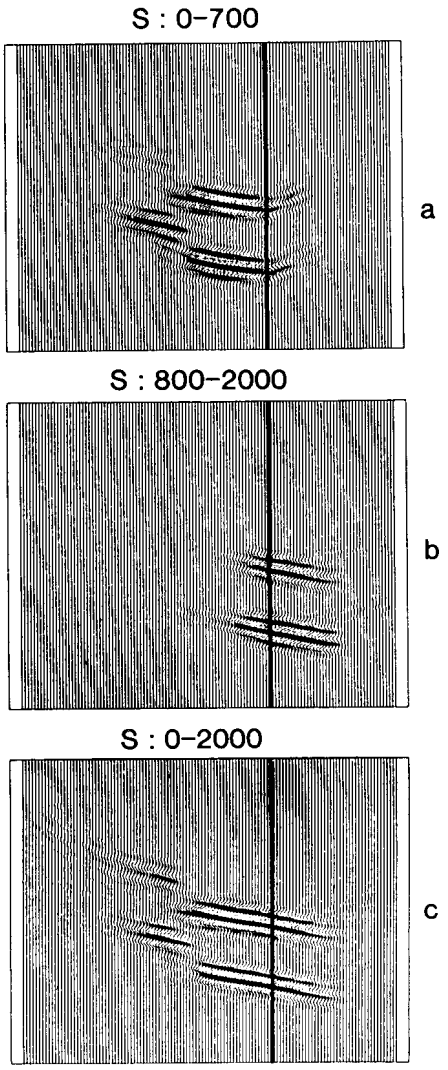

Fig. 12. Depth sections obtained by migrating and stacking VSP data sets: (a) sources left of the well (identical to Fig. 11); (b) sources right of the well; (c) sources at both sides of the well (superposition of a and b).

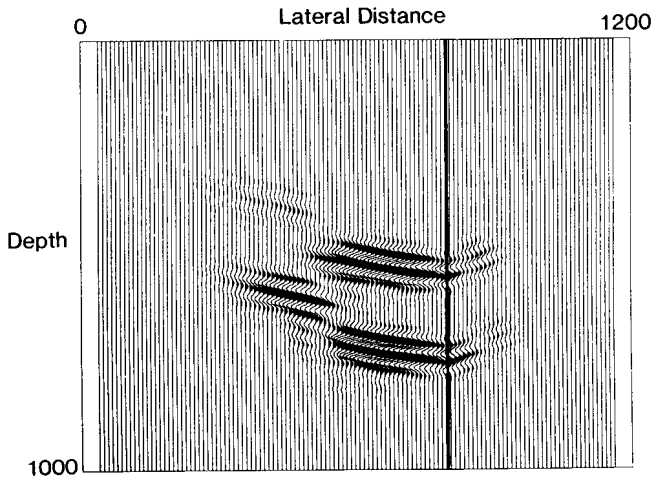

Fig. 11. Depth section obtained by migrating eight VSP data sets (with sources located from 0 to 700 m), followed by stacking.

with the wellhead at x = 700 m penetrates the subsurface across the pinch-out and the top of the anticline. Eleven VSP data sets were modelled by ray tracing, with sources located at positions from 0 to 1000 m with a spacing of 100 m. Figure 13a shows the rays from a source at x = 1000 m; Fig. 13b shows the corresponding VSP data set (upgoing waves only). Migration of each VSP data set, followed by stacking, yields the depth section shown in Fig. 14. Note that the reflectors are recovered mainly around the well. This can be easily understood if we keep in mind that most of the detected upgoing waves originate from those parts of the reflectors that are close to the well (see also Fig. 13a).

The last subsurface model contains four wells, penetrating faulted layers (Fig. 15). We modelled 11 VSP data sets for each well such that the overall reflector coverage is optimum. Figure 16 shows four depth sections, each of them obtained by migrating and

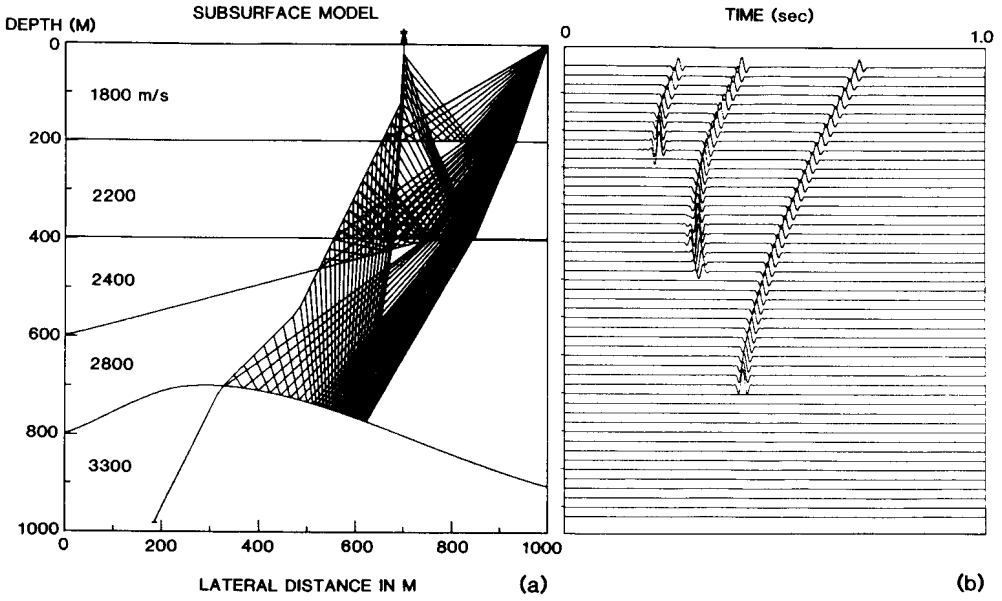

Fig. 13. (a) An inhomogeneous subsurface model with a deviated well. (b) VSP data set computed with ray tracing (source at 1000 m, wellhead at 700 m).

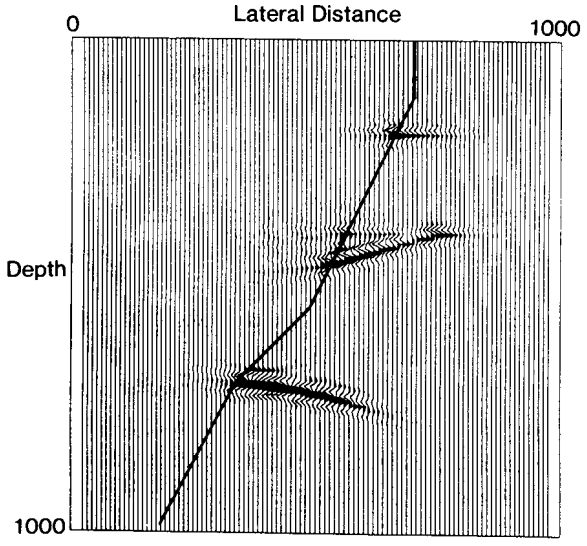

Fig. 14. Depth section obtained by migrating and stacking 11 VSP data sets with the sources located from 0 to 1000 m.

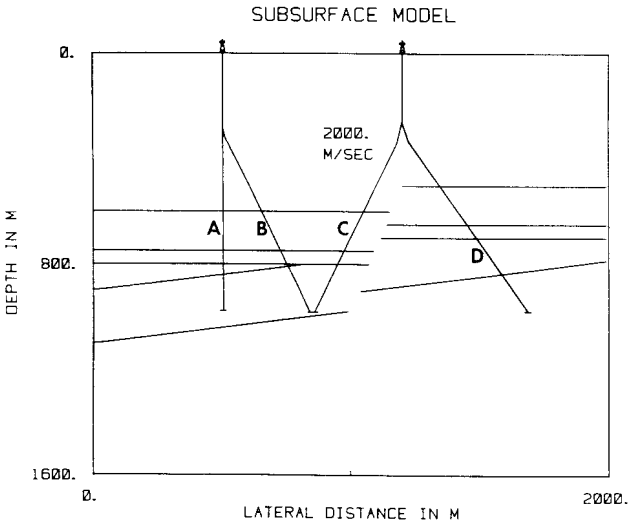

Fig. 15. Subsurface model containing four wells which penetrate faulted layers.

stacking the VSP data sets belonging to one well. Figure 17 shows the stack of the four depth sections of Fig. 16. Note that from this final result a great part of the subsurface structure can be recovered satisfactorily.

Future developments

The algorithm for VSP migration by single shot record inversion, as described in this paper, lends itself easily to some interesting modifications.

1. (a) The scheme can be extended for 3D applications by using 3D wavefield extrapolation operators. Because the downward extrapolation is carried out for each frequency component, the total amount of data to be handled simultaneously (a 2D array of complex numbers) is quite manageable. A good spatial resolution in all directions may be expected when VSP data from several wells below a 2D x,y grid are migrated and subsequently stacked.
   (b) In many practical situations seismic interpreters are mainly interested in an accurately positioned and well-resolved image of a pre-specified target zone. Therefore *target-oriented* migration (Wapenaar & Berkhout 1987) appears to be an accurate and

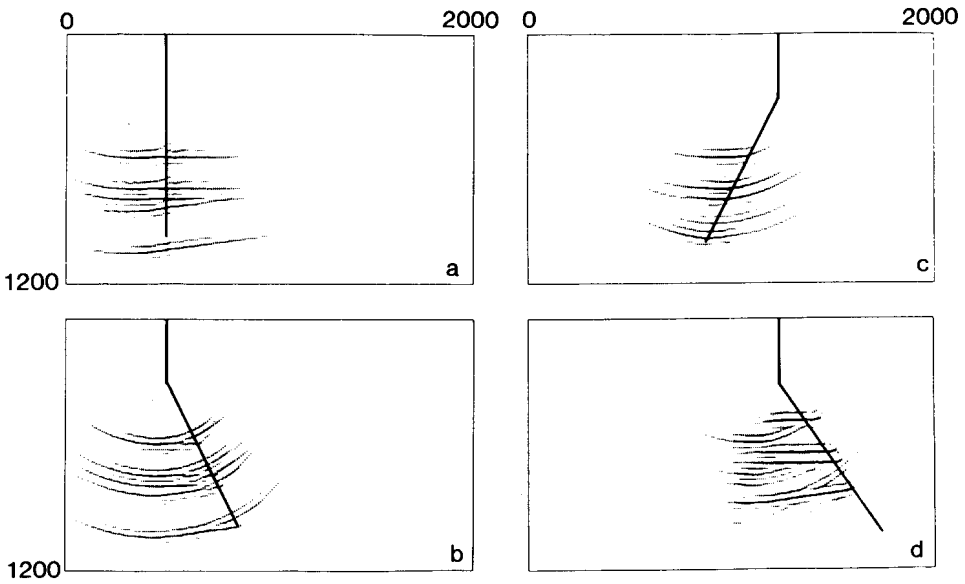

Fig. 16. Depth sections obtained by migrating and stacking 11 VSP data sets per well.

economically interesting solution for 3D migration of surface data as well as VSP data.

2. Independent one-way extrapolation of downgoing and upgoing waves may be replaced by simultaneous two-way wavefield extrapolation. In this way the algorithm may properly handle intra-bed multiple reflections. By using *full elastic* two-way wavefield extrapolation, wave conversion (from P to S and vice versa) may also be handled.
3. VSP migration by single shot record inversion is based on exactly the same principle as surface data migration by single shot record inversion (Berkhout 1984). In both techniques the individual migration results are stacked afterwards. Surface and VSP migration results can be easily combined (also by stacking afterwards), thus enhancing the spatial resolution of either one of the migration results.

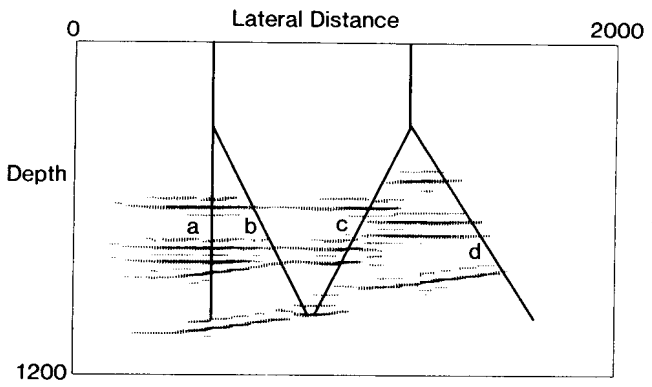

Fig. 17. Depth section obtained by stacking the migration results from the different wells (Fig. 16).

4. Throughout this paper it was assumed that the 'macro subsurface model' (a description of the subsurface in terms of the main geological boundaries with average velocities and/or velocity gradients of the macro layers) is known before the VSP migration is carried out. In practice one often starts by assuming a horizontally layered macro subsurface model with interval velocities obtained from a sonic log. The correctness of this model is then verified by comparing the direct source wave in the VSP data with a simulated direct source wave, modelled in the macro subsurface model. Unfortunately, even a perfect match of the measured and simulated source waves does not guarantee that the chosen macro subsurface model is correct. A more advanced procedure for verification of the macro model is based on the following principle. Given the source properties, *surface* data and a macro model, it is possible to generate VSP data simply by (acoustic or full elastic) two-way downward extrapolation of the total wavefield at the surface into the subsurface (for a 1D example see Wapenaar, Kinneging & Berkhout 1987). The advantage of this procedure is two-fold:
   (i) It allows very accurate macro model verification; if the generated VSP data are physically unacceptable (upgoing waves at smaller times than the downgoing source wave, etc.) then the chosen macro model is incorrect and a new macro model must be defined.
   (ii) It allows the simulation of VSP data from surface measurements. This capability may initiate entirely new processing techniques.

A further discussion of these modifications is beyond the scope of this paper. They are presently being investigated in Delft.

Conclusions

Structural subsurface information can be obtained from VSP data by migration. VSP migration is in general more complicated than surface data migration for the following reasons:

(i) Severe propagation velocity variations may occur along the recorded profile.
(ii) Steep propagation angles (relative to the normal to the borehole) may occur.
(iii) The acquisition configuration may be very irregular, particularly in the case of deviated wells.

We have discussed a VSP migration approach which is based on downward wavefield extrapolation and imaging for each basic experiment (shot record). We argued on theoretical grounds that the algorithm, which operates efficiently in the frequency domain, copes with all the above-mentioned problems. VSP migration experiments carried out with synthetic data demonstrate the validity of the scheme. Finally, the proposed approach may be extended for 3D applications as well as for the incorporation of multiple reflections and wave conversion.

Acknowledgments

We would like to thank Shell Companies in Indonesia for enabling the first author to carry out this project in Delft.

References

BALCH, A.H. & LEE, M.W. 1984. Vertical seismic profiling. International Human Resources Development Corporation.

BERKHOUT, A.J. 1984. Seismic migration: imaging of acoustic energy by wavefield extrapolation: B Practical aspects. Elsevier Science Publishing Company.

CHANG, W.F. & MCMECHAN, G.A. 1986. Reverse-time migration of offset vertical seismic profiling data using the excitation-time imaging condition. Geophysics 51, 67–84.

GAZDAG J. & SGUAZZERO, P. 1983. Migration of vertical seismic profiles by phase shift plus interpolation. Presented at the 45th Annual EAEG Meeting, Oslo.

HARDAGE, B.A. 1983. Vertical seismic profiling: Part A Principles. Geophysical Press.

HU, L.Z. & MCMECHAN, G.A. 1986. Migration of VSP data by ray equation extrapolation in 2D variable velocity media. Geophysical Prospecting 34, 704–734.

SEEMAN, B. & HOROWICZ, L. 1983. Vertical seismic profiling: separation of upgoing and downgoing acoustic waves in a stratified medium. Geophysics 48, 555–568.

WAPENAAR, C.P.A. & BERKHOUT, A.J. 1987. Three-dimensional target-oriented pre-stack migration. First Break 5, 217–227

WAPENAAR, C.P.A., KINNEGING, N.A. & BERKHOUT, A.J. 1987. Principle of pre-stack migration based on the full elastic two-way wave equation. Geophysics 52, 151–173.

Received 22 September 1986; accepted 9 February 1987.